GTP-24-1236

EXPERIMENTAL AND NUMERICAL INVESTIGATION OF $NH_3/H_2/N_2$ COMBUSTION IN A PREMIXED/STRATIFIED SWIRL BURNER

Jordan Davies
Cardiff University
Cardiff, UK

Luca Mazzotta
Sapienza University of Rome / Baker Hughes
Rome, Italy

Daisuke Sato
Cardiff University
Cardiff, UK

Syed Mashruk
Cardiff University
Cardiff, UK

Daniel Pugh
Cardiff University
Cardiff, UK

Domenico Borello
Sapienza University of Rome
Rome, Italy

Agustin Valera Medina
Cardiff University
Cardiff, UK

ABSTRACT

Interest in using renewably produced, partially cracked ammonia in gas turbines is gaining traction, but challenges relating to emissions of NO_x and unburned ammonia remain. The present work progresses existing research on using hydrogen stratification to reduce NO_x from ammonia/hydrogen flames by experimentally and numerically investigating the effects of also injecting nitrogen from the cracking process. It additionally assesses the NO_x reduction capability of a recently developed novel swirl burner by adding hydrogen to the stratified flow to maintain the diffusive equivalence ratio at two high NO production conditions, slightly lean and stoichiometric.

At slightly globally rich conditions, maintaining the diffusive equivalence ratio at 0.9 resulted in an order of magnitude reduction in NO emissions with only a 33% increase in unburned NH_3, compared to a fully premixed flame with the same fuel and air flow rates. This stratified configuration was found to increase consumption of NO by NH_2, likely due to flame morphology effects, while NO production from OH and HNO pathways was reduced. The reduced OH intensity was posited as the cause for increased NH_3 emission. A strong emissions sensitivity to diffusive equivalence ratio was found, as the case with a stoichiometric diffusive equivalence ratio did not show such marked improvements over its corresponding premixed condition. Both stratified and premixed flames were found to be stable, however stratification has potential to trigger instabilities at different frequencies to premixed.

Keywords: Ammonia, hydrogen, combustion, emissions, stratification, partial premixing.

NOMENCLATURE

Φ_D	Diffusive Equivalence Ratio
Φ_G	Global Equivalence Ratio
CFD	Computational Fluid Dynamics
CRN	Chemical Reactor Network
S_G	Swirl number
d	Diameter
RANS	Reynolds-Averaged Navier-Stokes
FGM	Flamelet Generated Manifold
PDF	Probability Density Function
TFSC	Turbulent Flame Speed Closure
PSR	Perfectly Stirred Reactor
PFR	Plug Flow Reactor
CRZ	Central Recirculation Zone
ERZ	External Recirculation Zone
ROP	Rate of Production
ROC	Rate of Consumption

1. INTRODUCTION

Renewably produced ammonia is considered a promising carbon-free energy vector due to its relative ease and low cost of storage and transportation compared to pure hydrogen [1]. Although these advantages are even greater if pure ammonia is used directly as a fuel, there are combustion challenges relating to its low reactivity and NO_x emissions [2,3].

Blending ammonia with other fuels to increase reactivity has been studied extensively. Mixing ammonia with methane or hydrogen has shown favourable improvements in burning velocity [4,5] and flammability limits [6]. Combustion with methane as part of the fuel will always result in carbon dioxide emissions, so mixing with hydrogen is the better option for decarbonisation. Furthermore, as ammonia has significant hydrogen content of ~18% on a mass basis [7], an

ammonia/hydrogen fuel blend can be achieved by partially cracking the ammonia immediately prior to combustion [8]. This has the added benefit of reducing cost by having to store only one fuel.

Numerous studies have also investigated NO_x mitigation strategies from ammonia/hydrogen fuel blends. Mashruk et al. demonstrated the NO_x emission dependence on ratio of ammonia to hydrogen [9], and the strong unimodal relationship between global equivalence ratio (Φ_G) and NO emissions, with a peak near Φ_G = 0.9 [6]. These studies noted that negligible NO_x emissions could be achieved at Φ_G = 1.2-1.3 due to NO consumption by NH_2 but resulted in significant unburned NH_3 emissions due to a decrease in the availability of H, O and OH radicals. They also showed significant N_2O emissions at lean conditions (Φ_G < 0.8) due to a reduction in flame temperature inhibiting N_2O consumption by free H atoms and shorter flames reducing residence time for the third-body reaction to act in [10,11,12]. N_2O is an important exhaust gas to monitor as it has a global warming potential roughly 250 times larger than carbon dioxide, meaning a flame with no CO_2 emissions but around 240ppm N_2O would have a similar global warming effect to a methane-air flame, as calculated in [13].

Recently, partially premixed ammonia/hydrogen combustion has received considerable attention to further reduce NO emissions. An NH_3/H_2 partially premixed concept was initially proposed and examined by Pugh et al. [14] at rich conditions. A diffusive flow of either NH_3 or H_2 was injected through a central lance with the main aim of creating local fuel-rich regions in the middle of the reaction zone. This resulted in a reduction in NO emissions but significant unburned NH_3 emissions were recorded. This study also examined the effect of elevated inlet pressures and temperatures more relevant to gas turbine conditions and reported an increase in NO emissions, particularly at rich conditions. As this is a complex nonmonotonic relationship depending on multiple variables, any kinetic mechanism selected for predicting emissions from pressurised stratified flames would require careful testing and validation. Franco et al. [15] proposed an alternative configuration for NH_3/H_2 flames, using two co-axial tubes, injecting fuel axially through the inner tube and air tangentially through the outer tube via a bluff body. However, the results presented by Franco et al. [15] did not deliver details of unburned ammonia, thus requiring further investigations. Mashruk et al. [16] recently presented a novel stratified combustion system that can operate in both premixed and stratified modes using ammonia/hydrogen blends. They observed that an increase in hydrogen stratification resulted in a reduction of NO and NO_2 emissions, but increased N_2O because of the reduced fuel in the premixed flow. It should be noted that the above works used only blends of ammonia, hydrogen and air, neglecting the nitrogen produced alongside the hydrogen in the cracking process.

The current work builds upon previous investigations by studying the influence of stratification in $NH_3/H_2/N_2$ flames utilising the same burner described by Mashruk et al. [16] at Cardiff University. Initially the premixed flow was maintained as a 20%$_{(vol.)}$ cracked ammonia blend and extra diffusive hydrogen was added to the stratified flow to preserve two set diffusive equivalence ratios (Φ_D), whilst varying the global equivalence ratio (Φ_G). Additionally, a numerical study using the CFD-CRN approach enabled a rate of production analysis to be carried out on the emissions results.

2. MATERIALS AND METHODS

This study assessed the NOx reduction capability of a recently commissioned burner system operating on a base blend of 20%$_{(vol.)}$ cracked ammonia ((66.7/25/8.3%$_{(vol.)}$ $NH_3/H_2/N_2$). Extra diffusive H_2 was injected into the stratified flow with the aim of promoting NO_x production, to aid in identifying mechanisms for NO_x reduction. In Case 1 Stratified, the extra diffusive H_2 flow rate was set to maintain the central diffusion flame at a slightly lean equivalence ratio (Φ_D = 0.9), known to produce peak NO emissions. For Case 1 Premixed, the same extra H_2 was instead added to the premixed flow, to offer a direct comparison. The global equivalence ratio was then varied 0.8 < Φ_G < 1.12. Addition of extra diffusive H_2 slightly varied the fuel blend, but this change was mirrored in the premixed configuration so comparisons could be drawn. This process was repeated in Case 2, but with the central diffusion flame maintained at stoichiometry (Φ_D = 1.0) to increase flame temperature. As Case 2 had a richer diffusive flame, the global equivalence ratio could be increased further, allowing 0.8 < Φ_G < 1.2 to be tested. As mentioned previously, operating at conditions leaner than Φ_G = 0.8 produces prohibitively high N_2O emissions and so was not investigated here. All experiments were conducted at a constant thermal power of 10kW.

2.1 Swirl Combustor

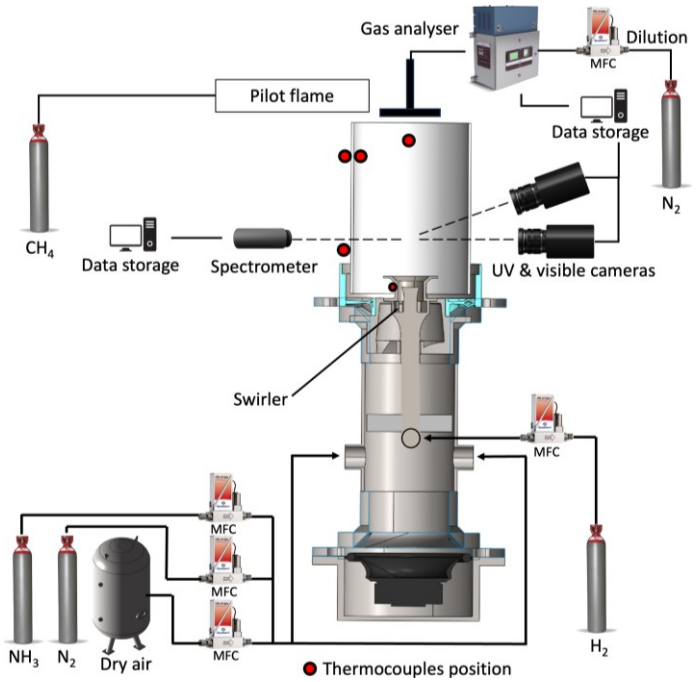

FIGURE 1: SCHEMATIC OF THE EXPERIMENTAL SETUP (NOT TO SCALE).

Experiments were conducted using an optically accessible radial-tangential swirl combustor (S_g = 1.05) shown in Figure 1 at atmospheric conditions (1.1 bar, and 288K).

Fuel and air were supplied using Bronkhorst mass flow controllers (± 0.5% between 15-95% of maximum flow). Figure 2 shows a diagram of the combustor architecture and flow paths. When operating in fully premixed mode, all H_2 was injected at the base of the swirler, mixing with NH_3, N_2 and air before flowing through the injector nozzle (d = 31.5mm), using a central injection lance (d = 22.5mm) as a bluff body. In stratified mode, the central injection lance was unblocked to allow some NH_3, N_2 and air through. Additionally, a portion of the H_2 was injected from the end of the central injection lance, ensuring the diffusion flame was maintained at either Φ_D = 0.9 or 1.0 to promote NO_x production. The global equivalence ratio Φ_G was calculated relative to the stoichiometric air-fuel ratio (AFR) as (Φ_G = total $AFR_{stoichiometric}$ / total AFR_{actual}), including both premixed and diffusive flows shown in Figure 2. The diffusive equivalence ratio Φ_D was calculated in the same manner but only considering the flow through the central injector.

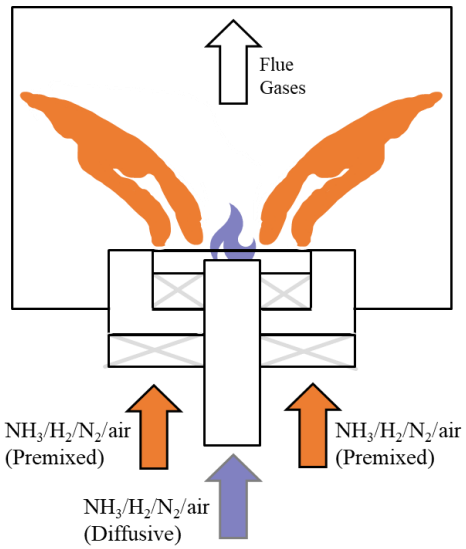

FIGURE 2: SIMPLIFIED DIAGRAM OF COMBUSTOR ARCHITECTURE.

To facilitate optical access for flame monitoring, chemiluminescence imaging and spectrometry, the flame was confined within a quartz glass tube (d = 156mm). The flame was monitored from a distance of 5m using a Logitech Brio camera.

2.2 Exhaust Gas Measurements

NO, NO_2, N_2O, NH_3, O_2 and H_2O were measured simultaneously using an Emerson CT5100 quantum cascade laser system. The cross-shaped sample probe with equidistant holes for homogenous sample collection was situated 25mm above the quartz tube outlet. Measured oxygen content was negligible at stoichiometric conditions, indicating no outside air was entrained into the sampling probe. The samples were carried to the gas analyser via a heated line, with measurements performed at 463K. For each condition, 120 samples were captured with a sampling rate of 1Hz (± 1% repeatability, 0.999 linearity), averaged, and normalised to dry 15% O_2 following equation 14 in [17]. Ongoing discussion surrounds this emission normalisation method [18], due to elevated water content in the exhaust of hydrogen-based fuels inflating dry ppmv values. However, as this paper focuses solely on cracked ammonia as a fuel, and no direct comparisons were drawn with carbon-based fuel, this method was deemed acceptable. For conditions where raw readings were above the analysers range, N_2 dilution was used (± 10% repeatability), as explained in detail in [11].

2.3 Chemiluminescence Measurements

OH* (309nm; $A^2\Sigma$-$X^2\Pi$ system), NH* (336nm $A^3\Pi$-$X^2\Sigma$ system) and NH_2* (630nm; single peak of NH_2 α band) images were captured simultaneously by multiple LaVision cameras each with a Sony ICX285AL sensor and Hamamatsu HB105831 intensifier and appropriate Edmund Optics bandpass filters as in [11]. The cameras recorded at a sampling frequency of 10Hz for a period of 20 seconds and the captured images were background corrected, 3x3 median filtered and averaged in Davis v10. The averaged chemiluminescence images then went through an Abel Deconvolution script in Matlab [19]. In this study, a positive correlation between ground state and excited radicals is assumed, as in [14,20].

An Avaspec-ULS4096CL spectrometer was used to capture broadband chemiluminescence intensity for a wide range of wavelengths, from 200-1100nm. It featured a 100µm slit and a 300 lines/mm grating, resulting in a full width half maximum resolution of 4.6nm. The spectrometer specified a 4096-pixel CMOS detector measuring 7 x 200µm, set to an exposure time of 1 second and averaged over 120 scans to improve the signal to noise ratio. Via a 600µm fibre optic cable, it was connected to a collimating lens for UV and visible light, mounted 30mm above the burner outlet and 240mm away from the central axis.

2.4 Pressure and Temperature Measurements

A water-cooled Kistler 211B6 pressure transducer mounted in the combustion chamber near the burner exit was used to measure combustor dynamics. Pressure fluctuations were measured at a sampling rate of 25kHz for a period of 20 seconds and then Fourier Transformed using a Matlab script for analysis.

The red dots in Figure 1 denote positions of R and K type thermocouples which had sampling rates of 1Hz and were averaged over a two-minute period for each operating condition.

2.5 CFD-CRN approach

The combination of Computational Fluid Dynamics (CFD) and Chemical Reactor Networks (CRNs) allows for the precise configuration of CRNs by discretising volumes accurately. This method is commonly used in analysing complex combustion processes like those in gas turbines [21] with relatively low computational cost and short processing times.

In this research, the CFD-CRN approach was applied to simulate and analyse the ammonia/hydrogen/nitrogen combustion. First, CFD was used to simulate a single test case,

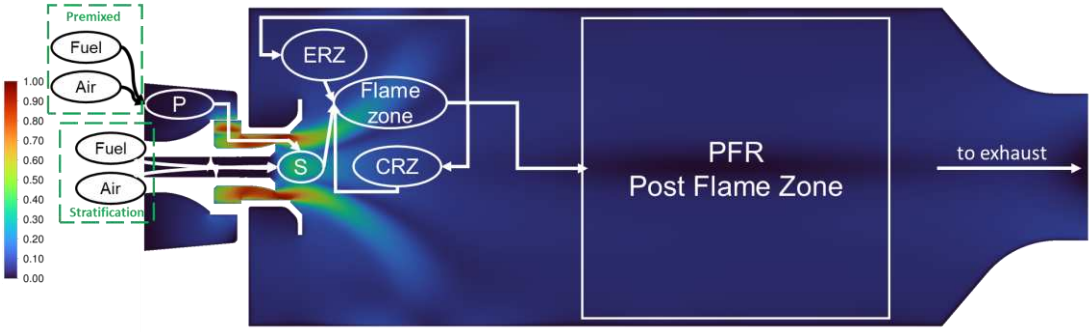

FIGURE 3: NORMALISED VELOCITY FIELD PREDICTED BY CFD SIMULATION. VOLUME DISCRETISATION AND ZONE DIVISION FOR CRN ANALYSIS.

obtaining temperature and velocity fields being crucial for defining different zones in the experimental setup. CRN numerical simulations of the flame were carried out using CHEMKIN-PRO. The CFD simulation was set up in ANSYS Fluent 2R2 using the Reynolds-Averaged Navier-Stokes (RANS) approach, to simulate one of the test points in the experimental campaign. A previous study [22] demonstrates that surrogate models can accurately predict NO_x emissions, temperature, and velocity fields. In this work, the burner's geometry is modelled using a three-dimensional (3D) computational domain, comprising a total of 6M polyhedral cells. The Realizable k-ϵ model with an enhanced wall function was the selected turbulence model. The Partially Premixed Combustion Model was implemented with the Flamelet Generated Manifold (FGM) approach [23]. The flamelets were carried out in Ansys Fluent, while the turbulence-chemistry interaction involved pre-integrating the look-up table with a β-PDF. The chemical kinetics from Otomo et al. [24] for the oxidation of ammonia-hydrogen flames, comprising 33 species and 213 reactions, was chosen for finite chemistry calculation. Zimont's Turbulent Flame Speed Closure (TFSC) [25] modelled the source term for the progress variable, defined as $c = Y_c/Y_{eq}$, where $Y_c = Y_{NO} + Y_{N_2} + Y_{H_2O} - Y_{H_2}$, and Y_{eq} is its equilibrium value. The laminar flame speeds included in the FGM combustion model were generated natively within Ansys Fluent after the boundary conditions were set and 1-D flamelets calculated. These laminar flame speeds were verified in CHEMKIN-PRO using the axisymmetric opposed-flow diffusion flame model by varying the equivalence ratio to account for the wide ranging degree of premixing present in a stratified flame. Figure 3 displays the axial velocity field with zone subdivisions characterising the Chemical Reactor Network (CRN). Four inlets of air, NH_3, H_2 and N_2 were used to feed two Perfectly Stirred Reactors (PSRs) considering Premixed (P) and Stratified (S) sections, respectively. Additionally, a PSR for the Flame zone and other two PSRs for Central Recirculation Zone (CRZ) and External Recirculation Zone (ERZ) were included. One Plug Flow Reactor (PFR) represented the flow zone where the velocity was completely axial. To validate temperature trends within the PSRs and PFR reactors in the CRN, a thermal analysis was carried out; Figure 4 shows the temperature field derived from CFD analysis. To determine the role of various reactions in changing NO emissions with stratification, absolute rate of production (ROP) values were calculated within the flame zone. The rate of consumption (ROC) is presented as a negative ROP, consistent with other studies [12]. Estimations of necessary heat loss were obtained from thermocouple measurements, located in appropriate positions in the burner.

FIGURE 4: NORMALISED TEMPERATURE DISTRIBUTION PREDICTED BY CFD SIMULATION.

3. RESULTS AND DISCUSSION

3.1 Effect of Stratification on Emissions

In Case 1 Stratified, extra diffusive H_2 was injected into the stratified flow to maintain $\Phi_D = 0.9$ to promote NO production. It was compared to Case 1 Premixed, where the extra diffusive H_2 was injected into the premixed flow.

The order of magnitude reduction in NO emissions seen in Figure 5 from Case 1 Stratified at $\Phi_G = 1.05$ can be explained by two main mechanisms, a reduction in NH and OH production and an increase in NO consumption by NH_2. HNO is an intermediary radical which can be formed from NH and OH radicals via the reaction shown in Equation 1.

$$NH + OH \leftrightarrow HNO + H \quad (1)$$
$$N + OH \leftrightarrow NO + H \quad (2)$$
$$NH + NO \leftrightarrow N2O + H \quad (3)$$

Figure 6 demonstrates the reduction in NO production for Case 1 Stratified via HNO radicals, as well as from OH radicals directly via Equation 2. Again, assuming a positive correlation between ground state and excited radicals, these numerical results were validated by the chemiluminescence images shown

in Figure 7. OH* intensity was found to be similar, but over a smaller flame volume, supporting lower NO production from routes consuming OH and HNO. Although OH* intensity can be directly correlated with changes in temperature, Figure 8 shows only small differences between the two configurations in the post flame zone.

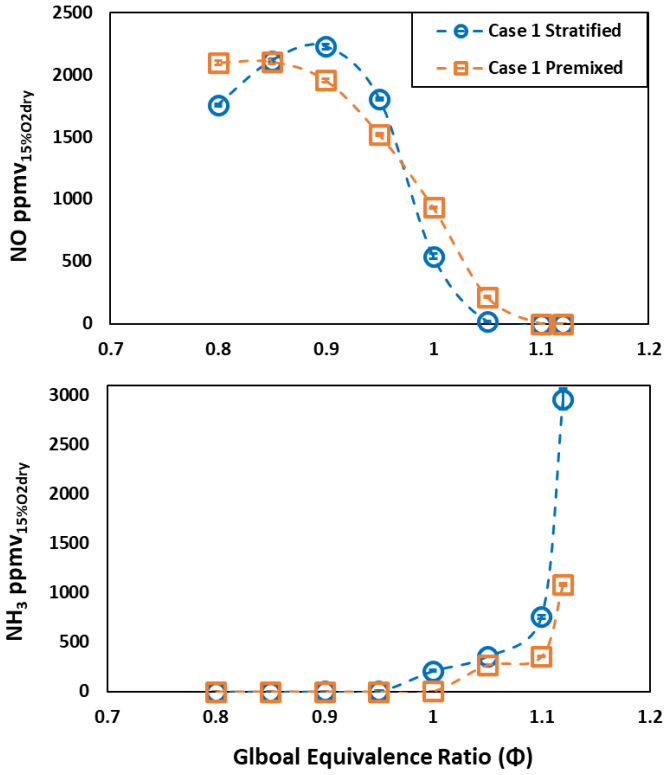

FIGURE 5: MEASURED EMISSIONS FROM CASE 1 WITH CHANGING GLOBAL EQUIVALENCE RATIO. NO (TOP) AND NH_3 (BOTTOM). (BEST-FIT LINES FOR CLARITY RATHER THAN MODELLED DATA).

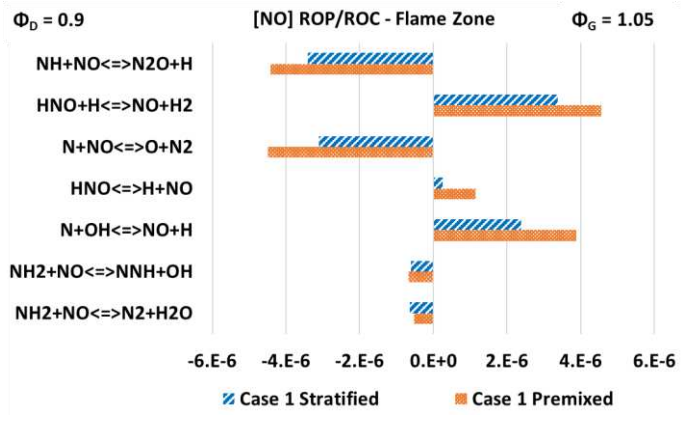

FIGURE 6: FLAME ZONE ABSOLUTE ROP/ROC [UNIT – MOLE/CM^3-SEC] FOR THE MOST SIGNIFICANT NO REACTIONS AT $\Phi_G = 1.05$ FOR CASE 1 STRATIFIED (BLUE) AND PREMIXED (ORANGE)

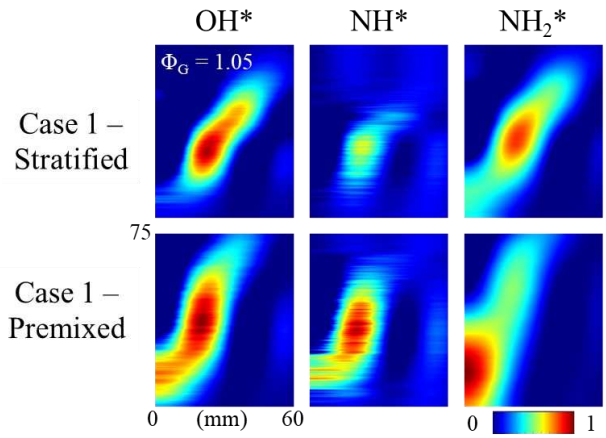

FIGURE 7: ABEL TRANSFORMED CHEMILUMINESCENCE IMAGES (OH*, NH* AND NH_2*) OF CASE 1 STRATIFIED (TOP) AND PREMIXED (BOTTOM) AT $\Phi_G = 1.05$. EACH SPECIES NORMALISED TO ITS CASE 1 $\Phi_G = 1.05$ MAXIMUM.

NH* intensity was significantly lower in Case 1 Stratified, again supporting lower NO production from routes consuming HNO. Compared to Case 1 Premixed, the stratified configuration showed less NO consumption by NH via the reaction shown in Equation 3, which would also suggest a reduction in N_2O emissions. Consistent with previous studies [9,12] most conditions produced negligible N_2O emissions due to the relatively high equivalence ratios examined here, and so N_2O was not plotted for brevity. However, at the leanest global equivalence ratio investigated ($\Phi_G = 0.8$), single digit ppmv (15% O_2 dry) N_2O values were measured for both Case 1 configurations, and the Stratified N_2O value was lower, further indicating the accuracy of the numerical investigation. NO_2 emissions followed the same general trend as NO and so were not plotted for brevity. The peak of 70ppmv (15% O_2 dry) NO_2 was found at the leanest conditions measured, with Case 1 Stratified slightly lower and both configurations reaching negligible readings by $\Phi_G = 1.0$.

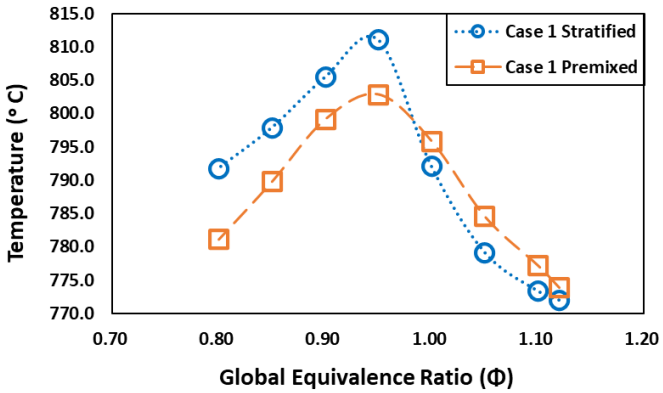

FIGURE 8: TEMPERATURE READINGS FROM A THERMOCOUPLE LOCATED IN THE CENTRE OF THE QUARTZ CONFINEMENT 50MM UPSTREAM OF THE OUTLET FOR CASE 1

The other mechanism by which Case 1 Stratified had lower NO emissions than Case 1 Premixed above stoichiometry was an increase in NO consumption by NH_2, from the reactions in Equations 4 and 5.

$$NH2 + NO \leftrightarrow NNH + OH \quad (4)$$
$$NH2 + NO \leftrightarrow N2 + H2O \quad (5)$$

These reactions do not immediately appear significant in Figure 6 until their contribution to the total NO consumption is considered. For Case 1, the contribution of these reactions was 35% larger in the stratified flame than in the premixed flame. Figure 7 shows Case 1 Stratified had slightly lower NH_2* intensity, centred farther away from the burner nozzle than Case 1 Premixed. This suggests less NH_2 was produced in the locally lean (Φ_D = 0.9) area near the central injector and was instead produced further downstream where the local equivalence ratio was more rich. This more spatially dispersed NH_2 would then have a longer residence time to consume NO produced in the area near the central injector and be available to consume NO in the ERZ.

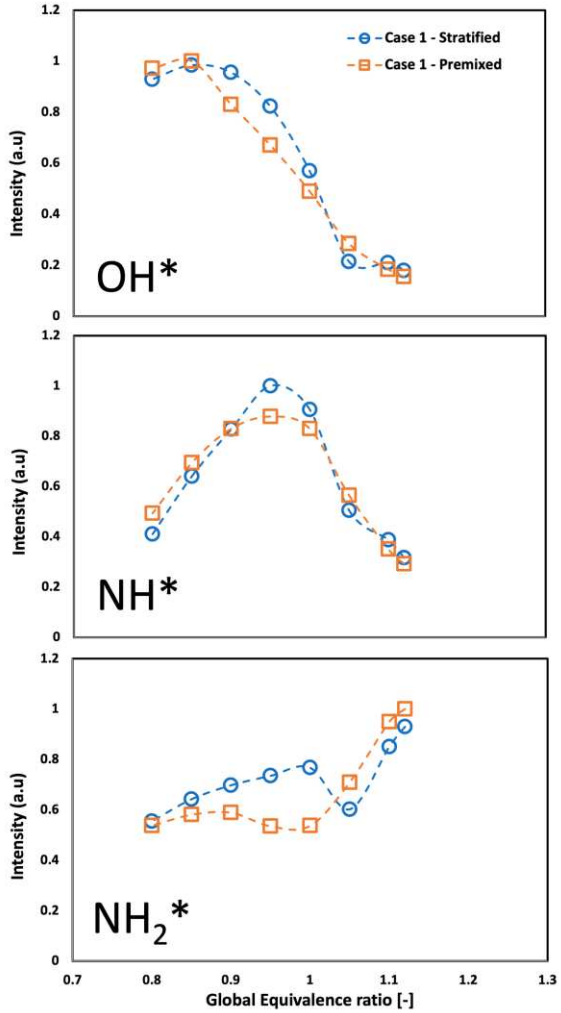

FIGURE 9: NORMALISED OPTICAL CHEMILUMINESCENCE SPECTROMETRY RESULTS FOR OH*, NH* AND NH_2*

Also shown in Figure 6, the thermal NO reactions of Equations 2 and 6 were slightly less significant in the stratified configuration than premixed for Case 1 at Φ_G = 1.05. This small reduction in significance of thermal NO reactions is reflected in the small reduction in temperature for the stratified configuration at rich conditions shown in Figure 8.

$$N + NO \leftrightarrow N2 + O \quad (6)$$

Unburned NH_3 emissions have previously been shown [26] to increase between $0.8 < \Phi_G < 1.2$ in fully premixed NH_3/H_2 flames due to reduced availability of OH radicals. This can explain the increase in NH_3 emissions shown in Figure 5 for Case 1 Stratified. Figure 7 does demonstrate a reduction in OH* intensity compared to Case 1 Premixed, but it is more clearly shown by the normalised chemiluminescence spectra intensity in Figure 9 at Φ_G = 1.05.

The approximately 15% increase in NO emissions from Case 1 Stratified shown in Figure 5 at slightly lean conditions can be attributed to the change in NH and OH production, consistent with when Φ_G = 1.05. However, the role of NH_2 in consuming NO was diminished, as expected from the lower NH_2* intensity at lean conditions shown in Figure 9. There was a smaller difference in NO emissions between the two configurations at lean conditions, which is reflected in Figure 10. However, some differences can still be seen. For example, both HNO and OH consumption to form NO were increased for Case 1 Stratified. Chemiluminescence data in Figures 9 and 11 support these numerical results by showing higher OH* intensity at Φ_G = 0.9. Figure 10 also shows the reduced significance of NH_2 in the NO consuming Equations 4 and 5, as there was less NH_2 available to be consumed in these reactions at globally lean conditions, compared to the globally rich conditions.

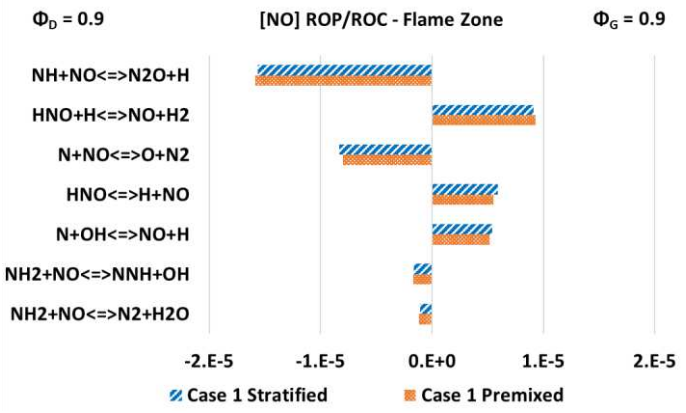

FIGURE 10: FLAME ZONE ABSOLUTE ROP/ROC [UNIT – MOLE/CM^3-SEC] FOR THE MOST SIGNIFICANT NO REACTIONS AT Φ_G = 0.9 FOR CASE 1 STRATIFIED (BLUE) AND PREMIXED (ORANGE)

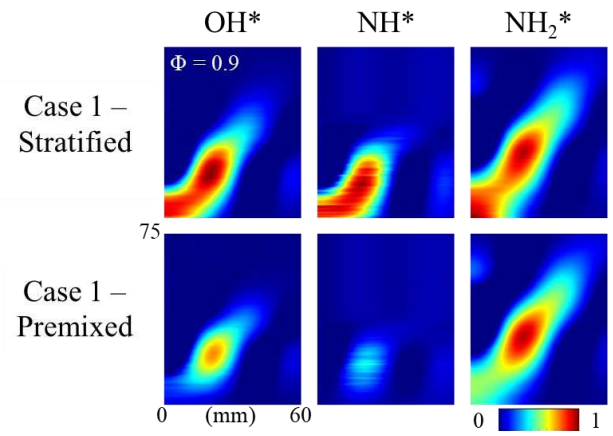

FIGURE 11: ABEL TRANSFORMED CHEMILUMINESCENCE IMAGES (OH*, NH* AND NH_2*) OF CASE 1 STRATIFIED (TOP) AND PREMIXED (BOTTOM) AT Φ_G = 0.9. EACH SPECIES NORMALISED TO ITS CASE 1 Φ_G = 0.9 MAXIMUM

Studies have shown that heat loss from the flame to the confinement walls can have a significant influence on emissions from ammonia flames, with wall quenching reducing NO emissions, but increasing N_2O and NH_3 emissions [27]. This is not the case in this study, demonstrated by two main reasons. First, Figures 7 and 11 show that although stratification did change the flame morphology, neither configuration caused the flame to impinge on the quartz glass confinement. The right-side edge of each chemiluminescence image is 60mm from the centreline of the flame, and the quartz tube is 18mm beyond that. The emissions data provides the second reason. Okafor et al. [27] reported N_2O and NH_3 emissions of 580ppmv and 4457ppmv at Φ_G = 0.8. Although this was from a pure ammonia flame and so not directly comparable to the current study, the fundamentals of ammonia combustion do apply. That is, emissions of unburned fuel at lean equivalence ratios represents a reduced combustion efficiency from excessive heat loss from the flame. That is not the case in the present study, proven by the negligible emissions of NH_3 at all conditions below stoichiometry, and the negligible or single digit ppmv emissions of N_2O at all conditions.

Both configurations in Case 1 reached negligible NOx emissions at a global equivalence ratio of 1.1, which is leaner than for NH_3/H_2 flames reported previously [9]. This is likely due to the N_2 present in the cracked ammonia fuel included in this study reducing reactivity and combustion efficiency. The combined emissions profile of Case 1 Stratified is particularly interesting at Φ_G = 1.05. Here, relatively low NO and NH_3 emissions of 20 and 358 ppmv (15% O_2 dry), respectively were found. This was an order of magnitude reduction in NO emissions with only a 33% increase in NH_3 emissions compared to the fully premixed configuration with the same total flow rates. In summary, this reduction in NO was a result of a reduction in NO production from OH and NH radicals, paired with an increase in NO consumption by NH_2. Lesser availability of OH radicals also resulted in an increase in unburned NH_3 emissions.

3.2. Effect of Varying Diffusive Equivalence Ratio

To investigate the effect of different central diffusion equivalence ratios, Φ_D was increased from 0.9 in Case 1, to 1.0 in Case 2. As in the previous section, the extra diffusive H_2 injected centrally in the stratified configuration was then injected into the premixed flow to provide baseline emissions for this fuel blend. As Case 1 had slightly different total flowrates to Case 2, the stratified configurations from each Case cannot be compared directly. It is however useful to compare the stratified configurations' relative difference from their respective premixed configurations.

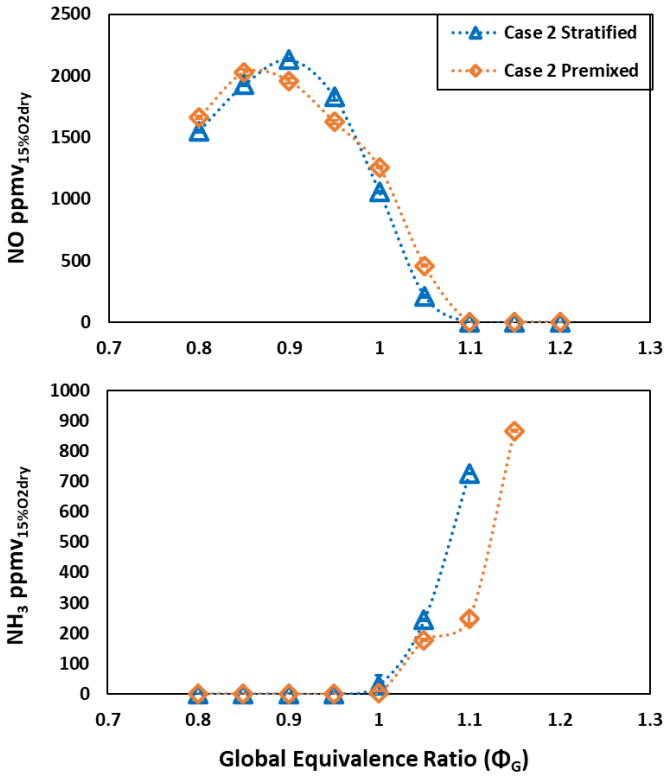

FIGURE 12: MEASURED EMISSIONS FROM CASE 2 WITH CHANGING GLOBAL EQUIVALENCE RATIO. NO (TOP) AND NH_3 (BOTTOM). OUT OF RANGE NH_3 AT RICH CONDITIONS NOT PLOTTED. (BEST-FIT LINES FOR CLARITY RATHER THAN MODELLED DATA).

Figure 12 shows that for Case 2, stratification with the diffusive flame maintained at a more rich equivalence ratio of Φ_D = 1.0 was less effective in reducing NO emissions than the Φ_D = 0.9 in Case 1. At Φ_G = 1.05, Case 2 Stratified had NO emissions roughly half that of the Case 2 Premixed, but 37% higher unburned NH_3, a poorer trade-off than found in Case 1. This was a significant difference from a relatively small change in flow rates, so numerical simulations were performed to clarify the mechanisms responsible, which were then compared with chemiluminescent data again assuming a positive correlation between the ground state and excited radicals. Figure 13 shows the differences in ROP/ROC between Case 2 Stratified and Premixed configurations was the same as for Case 1 in Figure 6,

but with smaller differences. This was expected as the differences between NO emissions was smaller.

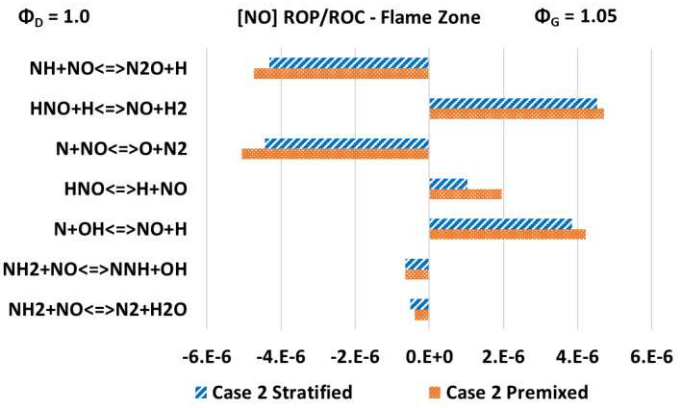

FIGURE 13: FLAME ZONE ABSOLUTE ROP/ROC [UNIT – MOLE/CM^3-SEC] FOR THE MOST SIGNIFICANT NO REACTIONS AT Φ_G = 1.05 FOR CASE 2 STRATIFIED (BLUE) AND PREMIXED (ORANGE)

Figure 13 shows a smaller relative difference in the ROP from reactions which consume HNO to form NO for Case 2 configurations. An explanation for this difference could be due to the stoichiometric diffusive flame having a higher local flame temperature near the central injector, increasing the availability of free H atoms to react with HNO. As NH and OH combine to form HNO via the reaction in Equation 1, a smaller difference in OH* and NH* could be expected between the Case 2 configurations when compared to the Case 1 configurations. This is demonstrated in Figure 14, where the NH* in particular has a similar intensity across the two configurations.

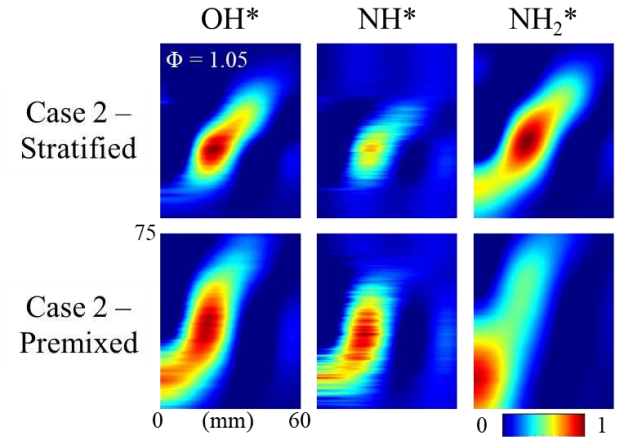

FIGURE 14: ABEL TRANSFORMED CHEMILUMINESCENCE IMAGES (OH*, NH* AND NH_2*) OF CASE 2 STRATIFIED (TOP) AND PREMIXED (BOTTOM) AT Φ_G = 1.05. EACH SPECIES NORMALISED TO ITS CASE 2 Φ_G = 1.05 MAXIMUM.

The other major difference shown in Figure 13 is the smaller De-NOxing impact of the NH_2 radicals in Equations 4 and 5. In Case 1, the contribution of these reactions in the stratified configuration was 35% larger than in the premixed configuration, but only 22% larger in Case 2. The difference in consumption of NH and NO from Equation 3 was similar for both Cases. This reduction in NH_2 significance could relate to the ratio of NO produced in the diffusive flame versus total NO produced. The peak NO production was found at Φ_G = 0.9, suggesting that Case 1 Stratified (Φ_D = 0.9) would produce more NO in the diffusive flame than Case 2 Stratified (Φ_G = 1.0). Compared to their respective premixed configurations, they should produce the same total emissions due to their total fuel and air flow rates being the same. However, Case 1 producing a larger percentage of that total NO in the region near the central injector would allow that NO more residence time to be consumed by the NH_2.

Figure 12 also shows a smaller increase in NO emissions at the lean conditions for Case 2 Stratified than was found for Case 1 Stratified. This was reflected in the ROP/ROC plot shown in Figure 15, where the only variation of significance was again in the HNO decomposition reaction. As in Section 3.1, NO_2 followed the same trend as NO. In Case 2, NO_2 peaked at a slightly lower value of 64ppmv (15% O_2 dry) at Φ_G = 0.8 and both configurations produced negligible readings at Φ_G = 1.0. N_2O emissions were negligible at all equivalence ratios tested and so neither are plotted here.

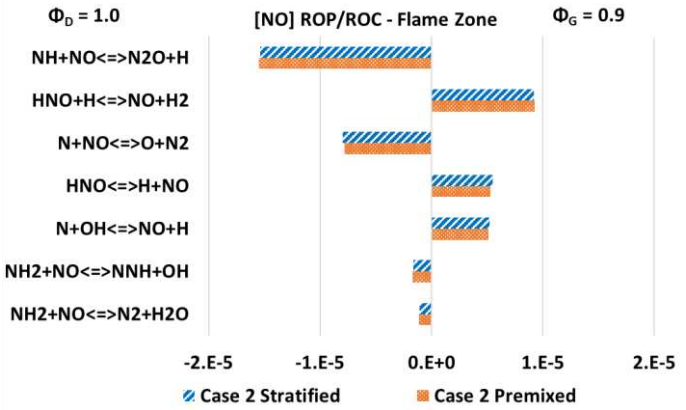

FIGURE 15: FLAME ZONE ABSOLUTE ROP/ROC [UNIT – MOLE/CM^3-SEC] FOR THE MOST SIGNIFICANT NO REACTIONS AT Φ_G = 0.9 FOR CASE 2 STRATIFIED (BLUE) AND PREMIXED (ORANGE)

To summarise, the stoichiometric central diffusion flame in Case 2 had a smaller effect on reducing NO emissions than the slightly lean one presented in Case 1. This is likely related to the stoichiometric diffusion flame having a locally higher temperature, increasing the availability of free H atoms to react with HNO and ultimately produce NO.

3.3. Effect of Stratification on Flame Stability

All tested configurations and conditions provided a stable flame, with no indication of lean or rich blowoff owing to all fuel blends being near stoichiometric. The dynamic pressure fluctuations within the quartz tube flame confinement were measured for all test conditions. However, as the same trends were observed for both Cases, only Case 1, which provided the best emissions performance is presented here.

Figure 16 shows the stratified configuration generally had lower RMS pressure fluctuations than the premixed configuration. The stratified case did not seem to possess the same sensitivity to equivalence ratio as the premixed and was comparatively constant at most test conditions.

It has been suggested that NH_2* can be used as a heat release marker in ammonia-based flames [20]. Figures 7 and 14 showed that stratification had a strong effect on flame morphology, with the NH_2* production being centred further downstream than in premixed configurations. This relocated centre of heat release could have changed the time delay and hence phase difference between the heat release fluctuations and pressure fluctuations to be out of phase, reducing the thermoacoustic instability in line with the Rayleigh Criterion [28]. The introduction of equivalence ratio fluctuations from stratification could also have affected the phase difference.

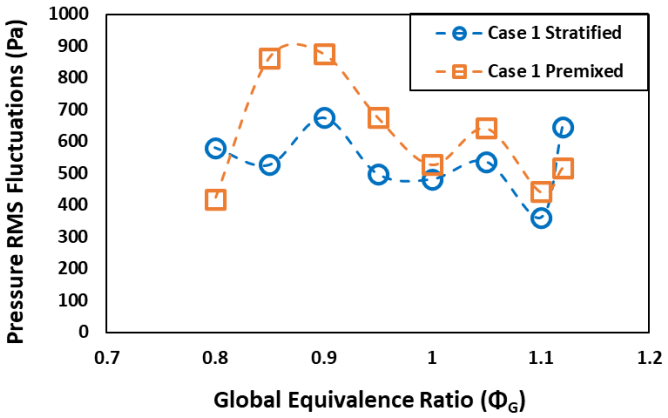

FIGURE 16: ROOT MEAN SQUARE FLUCTUATIONS IN COMBUSTOR PRESSURE WITH CHANGING GLOBAL EQUIVALENCE RATIO FOR CASE 1. (BEST-FIT LINES FOR CLARITY RATHER THAN MODELLED DATA).

Figure 17 shows the Fourier transformed pressure signal for the Case 1 test point with the best emissions performance (Φ_G = 1.05) above 50 Hz. Both configurations produced relatively high amplitude broadband combustion noise below 50 Hz of a similar magnitude, likely related to the injector geometry. There were however some significant differences at higher frequencies, so only those are presented and discussed here.

Both configurations experienced a significant pressure fluctuation at 95Hz and 251Hz, but stratification halved the amplitude when compared to the premixed configuration. Interestingly, the stratified configuration produced a peak at around 430Hz which is not present in the premixed data. This newly excited instability could have been triggered by equivalence ratio fluctuations that a stratified flame experiences, as a premixed flame only experiences velocity fluctuations. These instabilities are too low frequency to be associated with the natural frequency of the combustor, which was calculated to be the broadband signature around 630Hz present in both configurations.

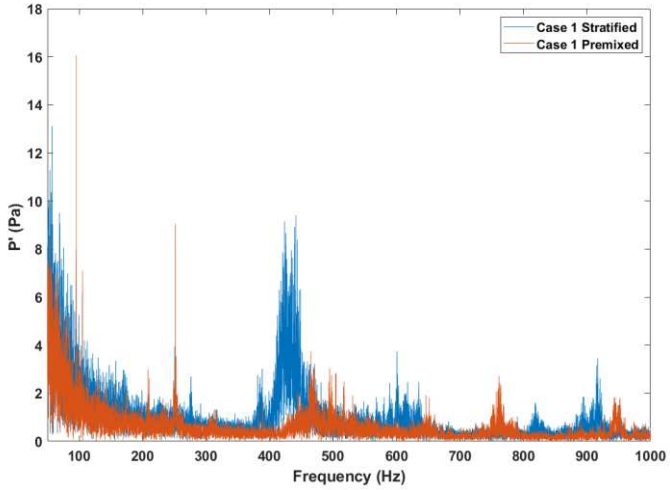

FIGURE 17: SPECTRAL COMPARISON OF CASE 1 STRATIFIED AND PREMIXED AT Φ_G = 1.05 ABOVE 50 HERTZ

4. CONCLUSIONS

The effect of supplying varying amounts of extra diffusive H_2 to the stratified flow of a 20% cracked ammonia flame was investigated using a turbulent swirl burner, at a constant thermal power of 10kW. Chemiluminescence data and numerical simulations were used to interpret changing emissions trends.

At stoichiometric and rich equivalence ratios, stratified configurations increased consumption of NO by NH_2, and reduced NO production from OH and HNO reaction pathways. The reduced OH intensity also resulted in an increase in unburned NH_3 emissions, which was offset by a significantly larger reduction in NO emissions. At slightly lean equivalence ratios, an increase in NO emissions was found, also due to changes in OH and NH production paired with diminished NH_2 intensity consuming less NO. Negligible N_2O was measured at all conditions as expected.

Emissions showed a strong sensitivity to the equivalence ratio of the stratified flow, related to diffusive flame temperature and NO – NH_2 residence times. Assuming an equal weighting for NO and unburned NH_3 emissions, the case where the diffusive flame had a slightly lean equivalence ratio showed better combined emissions performance.

Both examined configurations exhibited stable combustion. Whilst stratification generally reduced the amplitude of pressure fluctuations within the combustion chamber, it did also trigger new instabilities at different frequencies to the premixed flame which need to be properly assessed in further analyses.

ACKNOWLEDGEMENTS

This work was supported by the AMBURN project with funding from the Department for Energy Security and Net Zero (DESNZ) (Grant Number: IFS2-06-FLO), the EPSRC Centre for Doctoral Training in Resilient Decarbonised Fuel Energy Systems (Grant Number: EP/S022996/1), Reaction Engines Ltd and Sunborne Systems Ltd. The research was undertaken at Cardiff University's Thermofluids Lab (W/0.17) with invaluable technical support from Mr. Malcolm Seaborne. For the purpose of open access, the author has applied a CC BY public copyright licence to any Author Accepted Manuscript version arising.

REFERENCES

[1] Salmon, Nicholas, and Bănares-Alcántara, René. "Green Ammonia as a Spatial Energy Vector: A Review." *Sustainable Energy & Fuels* Vol. 5 No. 11 (2021): pp. 2814–39. https://doi.org/10.1039/D1SE00345C.

[2] Valera-Medina, Agustin., Xiao, Hua., Owen-Jones, Martin., David, William., and Bowen, Phillip. "Ammonia for Power." *Progress in Energy and Combustion Science* Vol. 69 (2018): pp. 63–102. https://doi.org/10.1016/J.PECS.2018.07.001.

[3] Kobayashi, Hideaki., Hayakawa, Akihiro., Somarathne, K. D. Kunkuma A., and Okafor, Ekenechukwu C. "Science and Technology of Ammonia Combustion." *Proceedings of the Combustion Institute* Vol. 37 No. 1 (2019): pp. 109–33. https://doi.org/10.1016/J.PROCI.2018.09.029.

[4] Okafor, Ekenechukwu C., Naito, Yuji., Colson, Sophie., Ichikawa, Akinori., Kudo, Taku., Hayakawa, Akihiro., and Kobayashi, Hideaki. "Experimental and Numerical Study of the Laminar Burning Velocity of CH4–NH3–Air Premixed Flames." *Combustion and Flame* Vol. 187 (2018): pp. 185–98. https://doi.org/10.1016/J.COMBUSTFLAME.2017.09.002.

[5] Shrestha, Krishna Prasad., Lhuillier, Charles., Alves Barbosa, Amanda., Brequigny, Pierre., Contino, Francesco., Mounaïm-Rousselle, Christine., Seidel, Lars., and Mauss, Fabian. "An Experimental and Modeling Study of Ammonia with Enriched Oxygen Content and Ammonia/Hydrogen Laminar Flame Speed at Elevated Pressure and Temperature." *Proceedings of the Combustion Institute* Vol. 38 No. 2 (2021): pp. 2163–74. https://doi.org/10.1016/J.PROCI.2020.06.197.

[6] Mashruk, Syed., Vigueras-Zuniga, Marco Osvaldo., Tejeda-del-Cueto, Maria Elena., Xiao, Hua., Yu, Chunkan., Maas, Ulrich., and Valera-Medina. Agustin. "Combustion Features of CH4/NH3/H2 Ternary Blends." *International Journal of Hydrogen Energy* Vol. 47 No. 70 (2022): pp. 30315–27. https://doi.org/10.1016/J.IJHYDENE.2022.03.254.

[7] Giddey, Sarbjit., Badwal, Sukhvinder., Munnings, Christopher., and Dolan, Michael., "Ammonia as a Renewable Energy Transportation Media." *ACS Sustainable Chemistry and Engineering* Vol. 5 No. 11 (2017): pp. 10231–39. https://doi.org/10.1021/ACSSUSCHEMENG.7B02219/ASSET/IMAGES/LARGE/SC-2017-02219T_0007.JPEG.

[8] Mei, Bowen., Zhang, Jianguo., Shi, Xiaoxiang., Xi, Zhongya., and Li, Yuyang. "Enhancement of Ammonia Combustion with Partial Fuel Cracking Strategy: Laminar Flame Propagation and Kinetic Modeling Investigation of NH3/H2/N2/Air Mixtures up to 10 Atm." *Combustion and Flame* Vol. 231 (2021): pp. 111472. https://doi.org/10.1016/J.COMBUSTFLAME.2021.111472.

[9] Mashruk, Syed, Kovaleva, Marina., Alnasif, Ali., Chong, Cheng Tung., Hayakawa, Akihiro., Okafor, Ekenechukwu C., and Valera-Medina, Agustin. "Nitrogen Oxide Emissions Analyses in Ammonia/Hydrogen/Air Premixed Swirling Flames." *Energy* Vol. 260 (2022): pp. 125183. https://doi.org/10.1016/J.ENERGY.2022.125183.

[10] Pugh, Daniel., Bowen, Phillip., Goktepe, Burak., Giles, Anthony., Mashruk, Syed., Valera-Medina, Agustin., and Morris, Steven. "Influence of Steam and Elevated Ambient Conditions on N2O in a Premixed Swirling NH3/H2 Flame*." Proceedings of the ASME Turbo Expo.* GT2023-102452. Boston, MA, June 26-30, 2023. http://asmedigitalcollection.asme.org/GT/proceedings-pdf/GT2023/86953/V03AT04A064/7043786/v03at04a064-gt2023-102452.pdf.

[11] Mashruk, Syed., Okafor, Ekenechukwu C., Kovaleva, Marina., Alnasif, Ali., Pugh, Daniel., Hayakawa, Akihiro., and Valera-Medina, Agustin. "Evolution of N2O Production at Lean Combustion Condition in NH3/H2/Air Premixed Swirling Flames." *Combustion and Flame* Vol. 244 (2022): pp. 112299. https://doi.org/10.1016/J.COMBUSTFLAME.2022.112299.

[12] Hayakawa, Akihiro., Hayashi, Masao., Kovaleva, Marina., Gotama, Gabriel J., Okafor, Ekenechukwu C., Colson, Sophie., Mashruk, Syed., Valera-Medina, Agustin., Kudo, Taku., and Kobayashi, Hideaki. "Experimental and Numerical Study of Product Gas and N2O Emission Characteristics of Ammonia/Hydrogen/Air Premixed Laminar Flames Stabilized in a Stagnation Flow." *Proceedings of the Combustion Institute* Vol. 39 No. 2 (2023): pp. 1625–33. https://doi.org/10.1016/J.PROCI.2022.08.124.

[13] Zhu, Xuren., Khateeb, Abdulrahman A., Guiberti, Thibault F., and Roberts, William L., "NO and OH* Emission Characteristics of Very-Lean to Stoichiometric Ammonia–Hydrogen–Air Swirl Flames." *Proceedings of the Combustion Institute* Vol. 38 No. 4 (2021): pp. 5155–62. https://doi.org/10.1016/J.PROCI.2020.06.275.

[14] Pugh, Daniel., Runyon Jon., Bowen, Phillip., Giles, Anthony., Valera-Medina, Agustin., Marsh, Richard., Goktepe, Burak., and Hewlett, Sally. "An Investigation of Ammonia Primary Flame Combustor Concepts for Emissions Reduction with OH*, NH2* and NH* Chemiluminescence at Elevated Conditions." *Proceedings*

of the Combustion Institute Vol. 38 No. 4 (2021): pp. 6451–59. https://doi.org/10.1016/J.PROCI.2020.06.310.

[15] Franco, Miguel C., Rocha, Rodolfo C., Costa, Mário., and Yehia, Mohamed. "Characteristics of NH3/H2/Air Flames in a Combustor Fired by a Swirl and Bluff-Body Stabilized Burner." *Proceedings of the Combustion Institute* Vol. 38 No. 4 (2021): pp. 5129–38. https://doi.org/10.1016/J.PROCI.2020.06.141.

[16] Mashruk, Syed., Alnasif, Ali., Yu, Chunkan., Thatcher, James., Rudman, James., Peronski, Lukasz., Meng-Choung, Chiong., and Valera-Medina, Agustin. "Combustion Characteristics of a Novel Ammonia Combustor Equipped with Stratified Injection for Low Emissions." *Journal of Ammonia Energy* Vol. 1 No. 1 (2023): pp. 21-32. https://doi.org/10.18573/JAE.10.

[17] British Standards Institute. "British Standard ISO 11042-1:1996, Gas Turbines. Exhaust Gas Emission Measurement and Evaluation" 1996. UK. https://www.iso.org/obp/ui/en/#iso:std:iso:11042:-1:ed-1:v1:en.

[18] Douglas, Christopher M., Shaw, Stephanie L., Martz, Thomas D., Steele, Robert C., Noble, David R., Emerson, Benjamin L., and Lieuwen, Timothy C. "Pollutant Emissions Reporting and Performance Considerations for Hydrogen-Hydrocarbon Fuels in Gas Turbines." *Journal of Engineering for Gas Turbines and Power* Vol. 144 No. 9 (2022): pp 0910031-7 https://doi.org/10.1115/1.4054949/6896265/GTP-22-1225.PDF.

[19] Mashruk, Syed. "Nitric Oxide Formation Analysis Using Chemical Reactor Modelling and Laser Induced Fluorescence Measurements on Industrial Swirl Flames" PhD Thesis. Cardiff University, Cardiff, UK. 2020. https://orca.cardiff.ac.uk/id/eprint/136590/.

[20] Mashruk, Syed., Xiao, Hua., Pugh, Daniel., Chiong, Meng Choung., Runyon, Jon., Goktepe, Burak., Giles, Anthony., and Valera-Medina, Agustin. "Numerical Analysis on the Evolution of NH2 in Ammonia/Hydrogen Swirling Flames and Detailed Sensitivity Analysis under Elevated Conditions." *Combustion Science and Technology* Vol. 195 No. 6 (2023): pp. 1251–78. https://doi.org/10.1080/00102202.2021.1990897.

[21] Chaturvedi, Shivansh., Santhosh, R., Mashruk, Syed., Yadav, Rajneesh., and Valera-Medina, Agustin. "Prediction of NOx Emissions and Pathways in Premixed Ammonia-Hydrogen-Air Combustion Using CFD-CRN Methodology." *Journal of the Energy Institute* Vol. 111 (2023): pp. 101406. https://doi.org/10.1016/J.JOEI.2023.101406.

[22] Mazzotta, Luca., D'Alessio, Francesco., Meloni, Roberto., Morris, Steve., Goktepe, Burak., Cerutti, Matteo., Romano, Christian., et al. "Modelling Ammonia-Hydrogen-Air Combustion and Emission Characteristics of a Generic Swirl Burner." *Journal of Engineering for Gas Turbines and Power* Vol. 146 No. 9 (2024): pp. 091022-11. https://doi.org/10.1115/GT2023-102803.

[23] Oijen, Jeroen van., and de Goey, Phillip. "Modelling of Premixed Laminar Flames Using Flamelet-Generated Manifolds." *Combustion Science and Technology* Vol. 161 No. 1 (2000): pp. 113–37. https://doi.org/10.1080/00102200008935814.

[24] Otomo, Junichiro., Koshi, Mitsuo., Mitsumori, Teruo., Iwasaki, Hiroshi., and Yamada, Koichi. "Chemical Kinetic Modeling of Ammonia Oxidation with Improved Reaction Mechanism for Ammonia/Air and Ammonia/Hydrogen/Air Combustion." *International Journal of Hydrogen Energy* Vol. 43 No. 5 (2018): pp. 3004–14. https://doi.org/10.1016/J.IJHYDENE.2017.12.066.

[25] Zimont, Vladimir., Polifke, Wolfgang., Bettelini, Marco., and Weisenstein, Wolfgang. "An Efficient Computational Model for Premixed Turbulent Combustion at High Reynolds Numbers Based on a Turbulent Flame Speed Closure." *Journal of Engineering for Gas Turbines and Power* Vol. 120 No. 3 (1998) pp. 526–32. https://doi.org/10.1115/1.2818178.

[26] Mashruk, Syed., Zitouni, Seif., Brequigny, Pierre., Mounaim-Rousselle, Christine., and Valera-Medina, Agustin. "Combustion Performances of Premixed Ammonia/Hydrogen/Air Laminar and Swirling Flames for a Wide Range of Equivalence Ratios." *International Journal of Hydrogen Energy* Vol. 47 No. 97 (2022): pp. 41170–82. https://doi.org/10.1016/J.IJHYDENE.2022.09.165.

[27] Okafor, Ekenechukwu C., Tsukamoto, Masaaki., Hayakawa, Akihiro., Somarathne, Kunkuma A., Kudo, Taku., Tsujimura, Taku., and Kobayashi, Hideaki. "Influence of Wall Heat Loss on the Emission Characteristics of Premixed Ammonia-Air Swirling Flames Interacting with the Combustor Wall." *Proceedings of the Combustion Institute* Vol. 38 No. 4 (2021): pp. 5139–46. https://doi.org/10.1016/J.PROCI.2020.06.142.

[28] Nicoud, Franck., and Poinsot, Thierry. "Thermoacoustic Instabilities: Should the Rayleigh Criterion Be Extended to Include Entropy Changes?" *Combustion and Flame* Vol. 142 No. 1–2 (2005): pp. 153–59. https://doi.org/10.1016/J.COMBUSTFLAME.2005.02.013.

List of Figure Captions

FIGURE 1: SCHEMATIC OF THE EXPERIMENTAL SETUP (NOT TO SCALE).

FIGURE 2: SIMPLIFIED DIAGRAM OF COMBUSTOR ARCHITECTURE.

FIGURE 3: NORMALISED VELOCITY FIELD PREDICTED BY CFD SIMULATION. VOLUME DISCRETISATION AND ZONE DIVISION FOR CRN ANALYSIS.

FIGURE 4: NORMALISED TEMPERATURE DISTRIBUTION PREDICTED BY CFD SIMULATIONS.

FIGURE 5: MEASURED EMISSIONS FROM CASE 1 WITH CHANGING GLOBAL EQUIVALENCE RATIO. NO (TOP) AND NH_3 (BOTTOM). (BEST-FIT LINES FOR CLARITY RATHER THAN MODELLED DATA).

FIGURE 6: FLAME ZONE ABSOLUTE ROP/ROC [UNIT – MOLE/CM^3 -SEC] FOR THE MOST SIGNIFICANT NO REACTIONS AT $\Phi_G = 1.05$ FOR CASE 1 STRATIFIED (BLUE) AND PREMIXED (ORANGE).

FIGURE 7: ABEL TRANSFORMED CHEMILUMINESCENCE IMAGES (OH*, NH* AND NH_2*) OF CASE 1 STRATIFIED (TOP) AND PREMIXED (BOTTOM) AT $\Phi_G = 1.05$. EACH SPECIES NORMALISED TO ITS CASE 1 $\Phi_G = 1.05$ MAXIMUM.

FIGURE 8: TEMPERATURE READINGS FROM A THERMOCOUPLE LOCATED IN THE CENTRE OF THE QUARTZ CONFINEMENT 50MM UPSTREAM OF THE OUTLET FOR CASE 1.

FIGURE 9: NORMALISED OPTICAL CHEMILUMINESCENCE SPECTROMETRY RESULTS FOR OH*, NH* AND NH_2*.

FIGURE 10: FLAME ZONE ABSOLUTE ROP/ROC [UNIT – MOLE/CM^3 -SEC] FOR THE MOST SIGNIFICANT NO REACTIONS AT $\Phi_G = 0.9$ FOR CASE 1 STRATIFIED (BLUE) AND PREMIXED (ORANGE).

FIGURE 11: ABEL TRANSFORMED CHEMILUMINESCENCE IMAGES (OH*, NH* AND NH_2*) OF CASE 1 STRATIFIED (TOP) AND PREMIXED (BOTTOM) AT $\Phi_G = 0.9$. EACH SPECIES NORMALISED TO ITS CASE 1 $\Phi_G = 0.9$ MAXIMUM.

FIGURE 12: MEASURED EMISSIONS FROM CASE 2 WITH CHANGING GLOBAL EQUIVALENCE RATIO. NO (TOP) AND NH_3 (BOTTOM). OUT OF RANGE NH_3 AT RICH CONDITIONS NOT PLOTTED. (BEST-FIT LINES FOR CLARITY RATHER THAN MODELLED DATA).

FIGURE 13: FLAME ZONE ABSOLUTE ROP/ROC [UNIT – MOLE/CM^3 -SEC] FOR THE MOST SIGNIFICANT NO REACTIONS AT $\Phi_G = 1.05$ FOR CASE 2 STRATIFIED (BLUE) AND PREMIXED (ORANGE).

FIGURE 14: ABEL TRANSFORMED CHEMILUMINESCENCE IMAGES (OH*, NH* AND NH_2*) OF CASE 2 STRATIFIED (TOP) AND PREMIXED (BOTTOM) AT $\Phi_G = 1.05$. EACH SPECIES NORMALISED TO ITS CASE 2 $\Phi_G = 1.05$ MAXIMUM.

FIGURE 15: FLAME ZONE ABSOLUTE ROP/ROC [UNIT – MOLE/CM^3 -SEC] FOR THE MOST SIGNIFICANT NO REACTIONS AT $\Phi_G = 0.9$ FOR CASE 2 STRATIFIED (BLUE) AND PREMIXED (ORANGE).

FIGURE 16: ROOT MEAN SQUARE FLUCTUATIONS IN COMBUSTOR PRESSURE WITH CHANGING GLOBAL EQUIVALENCE RATIO FOR CASE 1. (BEST-FIT LINES FOR CLARITY RATHER THAN MODELLED DATA).

FIGURE 17: SPECTRAL COMPARISON OF CASE 1 STRATIFIED AND PREMIXED AT Φ_G = 1.05 ABOVE 50 HERTZ.

